Wave forces on seawall walkway Darwin Luxury Hotel

By D Howe and I R Coghlan

WRL TR 2019/35, November 2019

UNSW Water Research Laboratory

UNSW SYDNEY

Water
Research
Laboratory
School of Civil and
Environmental Engineering

Wave Forces on Seawall Walkway Darwin Luxury Hotel

WRL TR 2019/35 | November 2019

By D Howe and I R Coghlan

Project details

Report title	Wave Forces on Seawall Walkway Darwin Luxury Hotel
Authors(s)	D Howe and I R Coghlan
Report no.	2019/35
Report status	Final
Date of issue	November 2019
WRL project no.	2019036
Project manager	I R Coghlan
Client	Wallbridge Gilbert Aztec RFP
Client address	Suite 7/9 Keith Lane Fannie Bay NT 0820
Client contact	Peter Brooks peter@rfpeng.com
Client reference	

Document status

Version	Reviewed by	Approved by	Date issued
Draft	M J Blacka	G P Smith	21 November 2019
Final	M J Blacka	G P Smith	27 November 2019

UNSW SYDNEY
Water Research Laboratory
School of Civil and Environmental Engineering

www.wrl.unsw.edu.au
110 King St, Manly Vale, NSW, 2093, Australia
Tel +61 (2) 8071 9800, ABN 57 195 873 179

bsi. ISO 9001 Quality Management

Contents

List of tables

List of figures

1 Introduction

The Water Research Laboratory (WRL) of the School of Civil and Environmental Engineering at UNSW Sydney was engaged by Wallbridge Gilbert Aztec (WGA) to determine the distribution of vertical wave forces on the underside of a cantilevered walkway slab on top of a proposed vertical seawall in Darwin (Figure 1-1). The proposed seawall is to be built along the foreshore to protect infrastructure associated with a new luxury hotel from erosion and wave overtopping. The walkway will provide the public with access to the foreshore seaward of the hotel. A wave return wall is to be located on the landward side of the walkway. An earlier wave return wall design was optimised for wave overtopping impacts on hotel infrastructure through previous physical model tests at the Queensland Government Hydraulics Laboratory (QGHL, 2017).

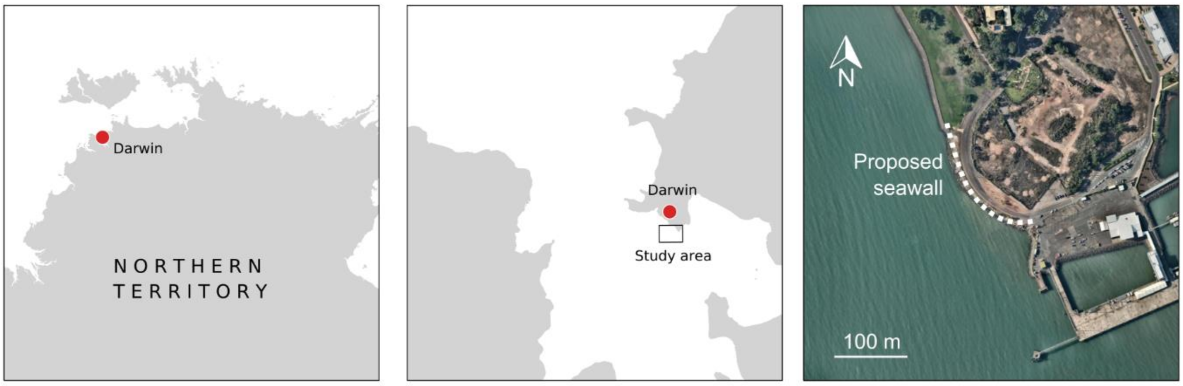

Figure 1-1 Location of study area (source: Nearmap)

WRL undertook two-dimensional (2D) physical modelling to measure the pressures and total force exerted upwards on the walkway for a range of water level, wave height and wave period combinations. A single scour level (eroded seabed level immediately adjacent to the seawall) was adopted for all tests. Since the design water levels are close to the walkway level, it was anticipated that the maximum wave loads would occur at a lower part of the tidal cycle when there is a greater potential for generation of "impulsive" type wave impact loads. The objective of the physical modelling investigation was to identify the peak pressures and forces on the underside of the cantilevered walkway for two (2) wave height-wave period combinations and the water levels at which they occur to assist with WGA's structural design.

This report summaries the physical model design, scaling, test program and findings of the study.

2 Model design

2.1 Testing facility

Two-dimensional testing was completed in the 1.2 m wave flume at WRL. This flume measures approximately 44 m in length, 1.2 m in width and 1.6 m in depth (Figure 2-1). The flume walls are constructed of rendered blockwork, with the exception of a glass panelled section where models are constructed, which allows visual observations to be made throughout testing. The permanent floor of the flume is constructed of concrete.

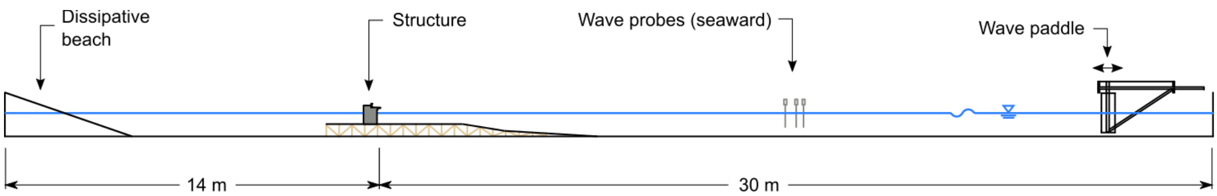

Figure 2-1 Schematic diagram of WRL 1.2 m flume (model scale)

The flume has a paddle-type wave generator powered by a 30 kW hydraulic piston system. The system is capable of generating both monochromatic and irregular wave spectra, with both wave types used in this investigation. The input signal is generated and fed to the wave paddle using a PC with WRL custom wave generation software.

The wave flume was filled with fresh water rather than salt water to avoid corrosion of the hardware and to simplify disposal of water after testing.

2.2 Scaling

2.2.1 Overview

Model scaling was based on geometric similarity between model and prototype, using an undistorted Froude scale of 15 (Table 2-1). Selection of the length ratio was primarily based on the upper limit wave height able to be generated in the 1.2 m wave flume. Forces and pressures had an additional scaling factor (N_γ) to adjust for the different fluid densities between the model (fresh water; 998 kg/m^3) and prototype (salt water; 1024 kg/m^3). All quantities are reported in prototype scale, unless otherwise noted.

Table 2-1 Froude scaling factors

Quantity	Unit	Froude relation	Scaling factor
Length	m	N_L	15
Time	s	$N_L^{1/2}$	3.87
Force	kN	$N_L^3 N_\gamma$	3,466
Pressure	kPa	$N_L N_\gamma$	51.41

2.2.2 Commentary on alternative scaling laws for force and pressure

Wave loads on vertical seawalls and their associated infrastructure (e.g. decks) can be divided between:

- Slowly acting loads, having durations of approximately 0.2 to 0.5 times a wave period, which are referred to as “pulsating” or “quasi-static” loads and are generally associated with non-breaking waves; and
- Short duration (approximately 0.01 times the wave period or less), high intensity loads, which are referred to as “impulsive” or “impact” loads and are generally associated with waves breaking directly on the structure which may entrap and compress an air pocket.

It is well accepted that “pulsating” or “quasi-static” loads can be scaled by the simple Froude relationships for force and pressure described in Table 2-1 with negligible scale effects (Cuomo et al., 2010). However, use of Froude scaling for “impulsive” loads may lead to over-estimation of force and pressure at prototype (real-world) scale and, unfortunately, a simple and reliable scaling relationship for short duration “impact” loads remains an unresolved problem which requires further research (Hydralab III, 2007).

Loading due to breaking waves is difficult to predict and the underlying processes are poorly understood, in part, because the shape of individual waves at impact determines the way in which air between the structure and the approaching wave is expelled, entrapped and/or entrained, which then influences the force and pressure generated (Bullock et al., 2004; 2007). If a wave overturns as it strikes a seawall, it can trap an air pocket, or if the wave has already broken, large quantities of air can be entrained so that a turbulent air-water mixture strikes a seawall. In both cases, the compressibility of the trapped or entrained air will affect the dynamics.

In a scale model, the compressibility of air is far less significant than in the prototype (real-world) since the increases in pressure above atmospheric are so much lower. Bullock et al. (2001) also found that model tests using fresh water waves entrained less air than salt water waves with similar geometry, resulting in comparatively higher peak impact pressures and shorter pressure rise times with fresh water. Since a two-phase fluid with greater air content is more compressible, it has been argued that impact pressures generated by salt water ocean waves will be lower than those predicted by Froude scaling of fresh water, scale laboratory experiments (Bullock et al., 2005). While entrained air content is less in physical models, the size of air bubbles is greater due to surface tension effects, making the extent of conservatism difficult to quantify (Hughes, 1993).

Most research on alternative scaling laws for force and pressure is focused on horizontal loads on vertical seawalls only (e.g. without a cantilevered walkway). Exceptions do exist though; Ramkema (1978) examined compression shocks that occur when air is trapped beneath a horizontal overhang protruding from a vertical wall. Using a physical model, Ramkema developed an alternative scaling law for impact pressures on the underside of an overhanging structure from air trapped by non-breaking standing waves. This law is only applicable for scaling instantaneous peak values, not whole test time series. However, Ramkema warned that the alternative scaling law for pressure may not be applicable to the case of compression impacts caused by breaking waves (as is the case with Darwin seawall).

During the design storm events modelled for the Darwin seawall, individual waves generated both “pulsating” and “impulsive” vertical loads on the underside of the cantilevered walkway. In the design of this model, WRL adopted the recommendations of key physical modelling guidelines (Hughes, 1993 and HYDRALAB III, 2007) for minimising scale effects on vertical seawall structures by maximising the model scale and the data acquisition rates for force and pressure. While it is acknowledged that alternative scaling laws which provide less conservatism exist, WRL has universally adopted Froude scaling for wave-generated force and pressure as it will provide conservative results for WGA's subsequent structural design. For a process known to contain unresolved scientific uncertainties, we consider that this a reasonable application of the precautionary principle.

2.3 Model construction

2.3.1 Bathymetry

Bathymetry measurements directly offshore of the proposed vertical seawall were not available for analysis by WRL. In their absence, the seabed geometry adopted (Figure 2-2) was identical to that tested previously at the Queensland Government Hydraulics Laboratory (QGHL, 2017) as accepted by WGA. The location where this bathymetry transect was extracted within the proposed structure footprint and its direction is unknown to WRL. The only change was that the scour level at the seawall was raised from -4.0 m AHD to -3.5 m AHD on the basis of advice from WGA (McMahon Services, 2019) from three (3) boreholes drilled at the site. WRL continued the 1V:6.2H slope adopted by QGHL seaward of the eroded flat from -4.0 m AHD to -3.5 m AHD to fill in the resulting "gap" in the bathymetry. Note that while all tests were conducted with a scour level of -3.5 m AHD, it is conceivable that similar peak forces and pressures on the underside of the cantilevered walkway may occur for higher scour levels. This is an important consideration for the asset owner; extreme uplift loads may still occur with higher sand levels at the vertical seawall.

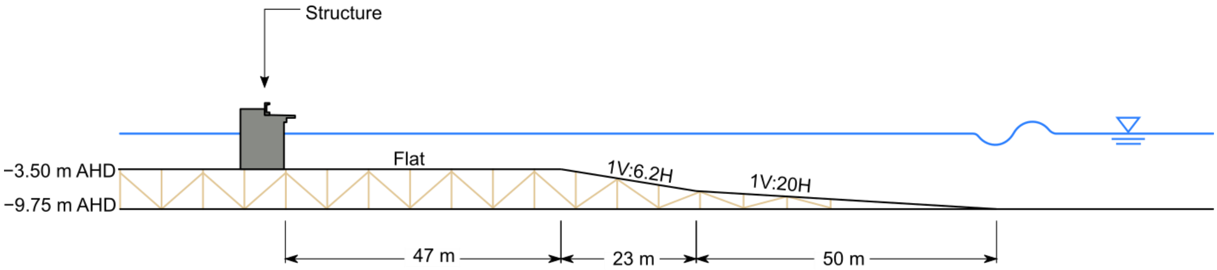

Figure 2-2 Model bathymetry and structure (prototype scale)

The bathymetric profile adopted for the modelling was constructed as a false, elevated floor within the wave flume. The false floor was constructed from water-resistant plywood (Figure 2-3) with the following characteristics:

- Flat bathymetry extended 47 m from the toe of the model at an elevation of -3.5 m AHD;
- The bathymetry followed a 1V:6.2H slope from -3.5 m AHD to -7.26 m AHD;
- Seaward of -7.26 m AHD the false floor sloped at 1V:20H to intersect the permanent flume floor at -9.75 m AHD, consistent with Hydralab III (2007) modelling guidelines.

Figure 2-3 Construction sequence for 2D model bathymetry

The Hydralab (2007) guidelines for physical modelling of coastal structures usually recommend that at least three (3) wavelengths of bathymetry be constructed seaward of the model structure. However, in special cases (e.g. small wave height to water depth ratios) modelling of the bathymetry can be neglected. This is the case for the upper water levels tested on the Darwin seawall. Some bathymetry was required to be constructed to allow sufficient water depth at the wave paddle to produce the required wave heights (e.g. the model seawall needed to be raised up off the permanent floor of the flume). At the beginning of the test program, it was unknown how far below the design water levels would need to be tested to identify the peak pressures and forces on the underside of the cantilevered walkway. For the range of conditions tested, the 120 m length of bathymetric profile seaward of the Darwin seawall model corresponded to 1.6 (5.6 m AHD water level) to 2.1 (2.0 m AHD water level) wavelengths. For the lower water level tests that required a bathymetry, only reproducing approximately 2 wavelengths rather than the recommended 3 wavelength is considered reasonable because the bathymetry within 1-2 wavelengths of the structure has the greatest influence on the wave climate and loading conditions at the structure (Hydralab, 2007; Van Gent and Giarrusso 2005).

2.3.2 Vertical seawall

The majority of components of the vertical seawall were also constructed from water-resistant plywood. The wave return wall on the landward side of the walkway was constructed from painted timber and the capping beam was constructed from painted PVC plastic sheet. All dimensions were consistent with Section 1 on the design drawing provided by WGA (Robert Bird Group, 2018; reproduced in Appendix A) except that, as agreed with WGA, the proposed piles in the prototype were constructed as a simplified smooth vertical wall in the physical model and the balustrade at the seaward edge of the walkway was omitted. The future earthworks level landward of the wave return wall was 6.5 m AHD and, as discussed in Section 2.3, the scoured bed level adjacent to the seawall was assumed to be -3.5 m AHD.

2.4 Instrumentation

A combination of capacitance wave probes, load cells, and pressure sensors were used during testing (Table 2-2, Figure 2-4, Figure 2-5). The accuracy of these types of sensors is typically in proportion to the overall measurement range of the sensor, and the instruments are typically selected to have a capacity slightly larger than the expected loads, so as to maximise the accuracy of the measurements obtained. However, in this case preliminary estimates of maximum wave height, uplift force and pressure were not available at the time of model design, and as such WRL relied on previous experience from modelling of similar coastal structures to select the most appropriate instrumentation. The instrument signals were recorded on a PC using a National Instruments data acquisition card and WRL data acquisition software. High-speed oblique videos were recorded for each test.

Table 2-2 Instruments used in testing

Instrument	Quantity	Sample rate[1] (Hz)	Measurement Range[1]	Noise[2]
Wave probe	Wave characteristics	13	0 to 6.75 m wave height	<±1%
Load cell	Uplift forces	258	-1.73 to 1.73 MN (individual) -6.93 to 6.93 MN (total)	<±1%
Pressure sensor	Uplift pressures	258	-150 to 700 kPa	<±0.5%

1. Prototype (real-world) scale.
2. Static instrument noise compared to typical measurement values.

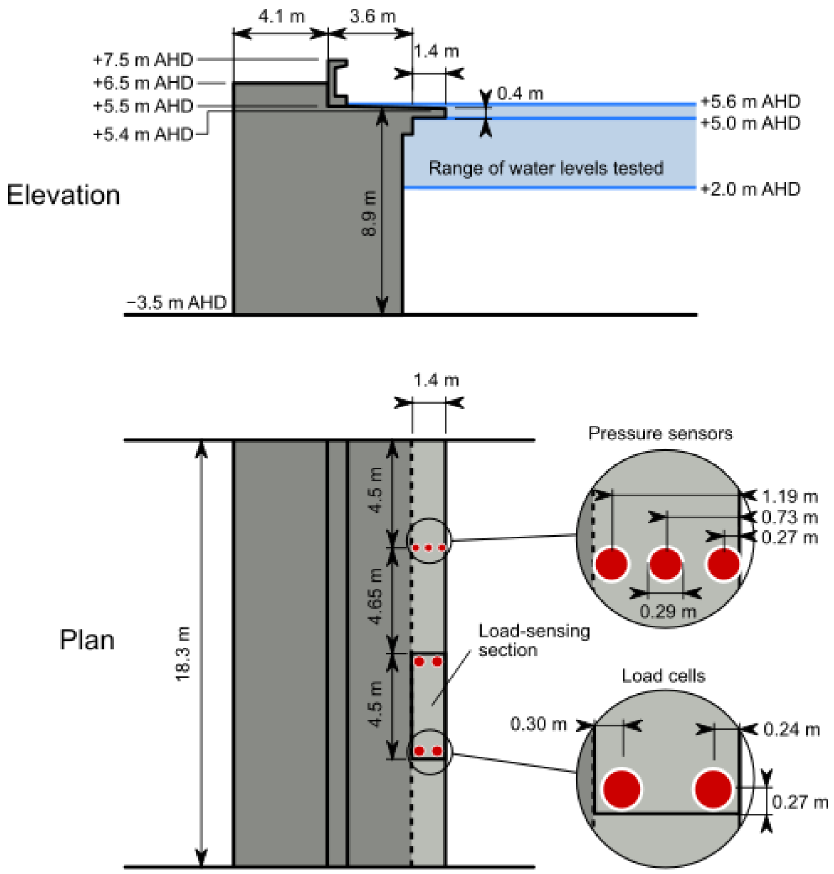

Figure 2-4 Model instrumentation and dimensions (prototype scale)

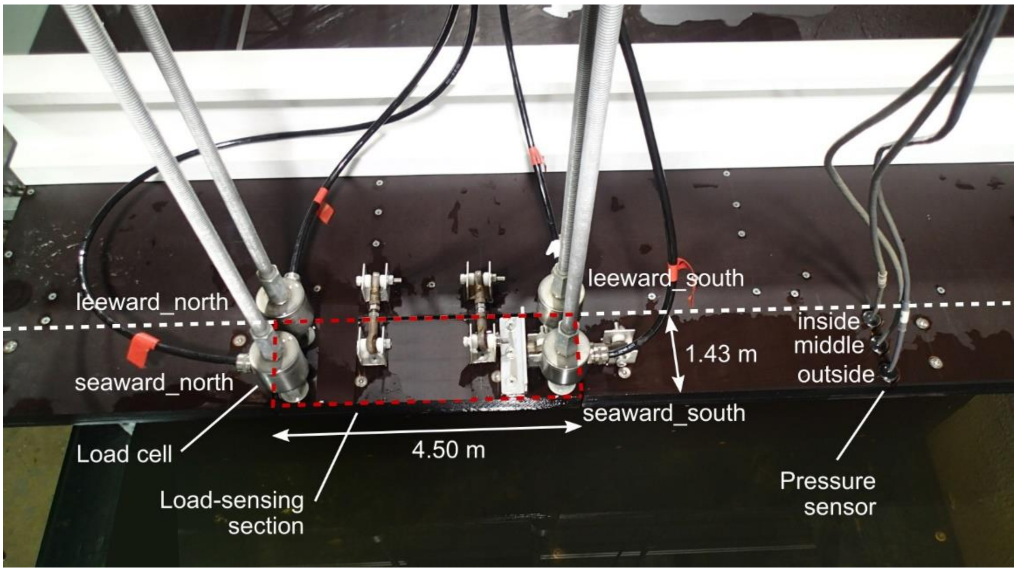

Figure 2-5 Top-view photograph of model sensor arrangement (dimensions in prototype scale)

A static calibration was performed on each instrument to ensure it was operating correctly across its full measurement range.

An additional dynamic in-situ “pull test” was completed for the load cells, to quantify mechanical losses in the load-sensing section of the structure, and to verify that all forces were being correctly distributed through the instrument rig. The extent of instrumentation noise relative to typical loads measured in the wave flume was also assessed during the “pull test”. Finally, a mass damper was added to the load cell set up and one wave test repeated on the model seawall structure to assess the extent of resonance within the test rig. On the basis of these sensor-setup verification tests, a 10% uncertainty factor was applied to all force measurements to allow for accuracy limitations in the model setup (i.e. all reported forces have been multiplied by 1.1).

2.5 Wave climates

Two different cyclonic design conditions were identified by BMT WBM (2017 and 2018; Table 2-3) and provided by WGA to WRL for the testing.

Table 2-3 Design conditions

Description	SWL (m AHD)	H_s (m)	T_p (s)
Design condition 1	5.0	2.6	8.1
Design condition 2	5.6	2.0	8.7

Two irregular drive signals were generated using a JONSWAP spectrum, each with 1,000 waves to be statistically relevant (Table 2-4).

Table 2-4 Drive signals used in testing

Wave Condition	No. waves	Duration	H_s (m)	T_p (s)
1	1,000	2 h 25 min	2.6	8.1
2	1,000	2 h 15 min	2.0	8.7

Two more lower water levels (2.75 m AHD and 4.0 m AHD) were included in addition to those in Table 2-3, to allow more space for waves to impact with the underside of the structure and potentially develop high uplift forces. The two (2) different drive signals and four (4) water levels yielded eight (8) different wave climates (Table 2-5). The wave climates were calibrated with the bathymetry installed in the flume, but with the structure removed, to minimise wave reflections. The four (4) calibrated drive signals for each wave condition were used to determine the required drive signal gains by interpolation for other test water levels.

Note that wave condition 1 was tested at a water level of 5.6 m AHD (0.6 m above its design water level) as was done by QGHL (2017).

The tested wave height and period for both wave conditions was unchanged for all water levels tested. It is acknowledged that this assumption may be conservative as the wave height may be lower below the design water level in the lower part of the tidal cycle (i.e. concurrent peak wave height and water level during the two (2) design cyclones).

Waves were measured using two (2) different three-probe arrays: one in deep water offshore; and one at the structure (Figure 2-1). Incident and reflected irregular wave trains were separated using the Mansard and Funke (1980) method during post-processing analysis. Reported wave statistics are based on the incident waves observed at the structure.

Table 2-5 Calibrated wave climates

SWL (m AHD)	Target		Observed	
	Hs (m)	Tp (s)	Hs (m)	Tp (s)
2.75	2.6	8.1	2.6	8.1
	2.0	8.7	2.0	8.6
4.0	2.6	8.1	2.6	8.2
	2.0	8.7	2.0	8.7
5.0	2.6	8.1	2.7	8.2
	2.0	8.7	2.0	8.7
5.6	2.6	8.1	2.6	8.3
	2.0	8.7	2.0	8.6

2.6 Test program

A total of 19 tests were completed (Table 2-6) to identify the water level (to within 0.1 m) at which the peak pressure and force occurred for both wave conditions. Tests were repeated at different water levels to determine the worst conditions for uplift forces and pressures. During testing, it became apparent that the maximum uplift forces were observed when the water level was between 2.4 m AHD and 3.0 m AHD. As no wave climates had been calibrated at those water levels, the required drive signal gain was estimated based on the results of the wave climate calibration that had been previously completed. For these uncalibrated tests where the required drive signal gains were derived by interpolation, it has been assumed that the wave statistics were approximately equal to their target values.

Table 2-6 Test program

Drive signal	Test number	Calibrated[1]	SWL (m AHD)	H_s (m)	T_p (s)
1	4		2.0	2.6	8.1
	7		2.25	2.6	8.1
	9		2.4	2.6	8.1
	6		2.5	2.6	8.1
	8		2.6	2.6	8.1
	3	✔	2.75	2.6	8.1
	5		3.0	2.6	8.1
	2		3.5	2.6	8.1
	1	✔	5.6	2.6	8.1
2	19		2.0	2.0	8.7
	10		2.5	2.0	8.7
	16		2.65	2.0	8.7
	11	✔	2.75	2.0	8.7
	17		2.82	2.0	8.7
	14		2.9	2.0	8.7
	12		3.0	2.0	8.7
	15		3.1	2.0	8.7
	13		3.5	2.0	8.7
	18	✔	5.6	2.0	8.7

1. Drive signal was calibrated before testing. For uncalibrated tests, the required gain of the input drive signal was estimated, therefore the wave statistics are approximate.

3 Results

3.1 Video records

The oblique video footage was used to describe the behaviour of waves at different water levels (Table 3-1, Figure 3-1).

Table 3-1 Qualitative descriptions of waves at different water levels

Water level	Wave breaking	Overtopping of crown wall	Degree of uplift slamming on cantilevered walkway
Low (< 2.25 m AHD)	Offshore	None	Moderate
Intermediate	Onto structure	Extensive spray, and some green water on larger waves	Violent
High (> 5 m AHD)	Over structure	Green water for most waves	Minimal

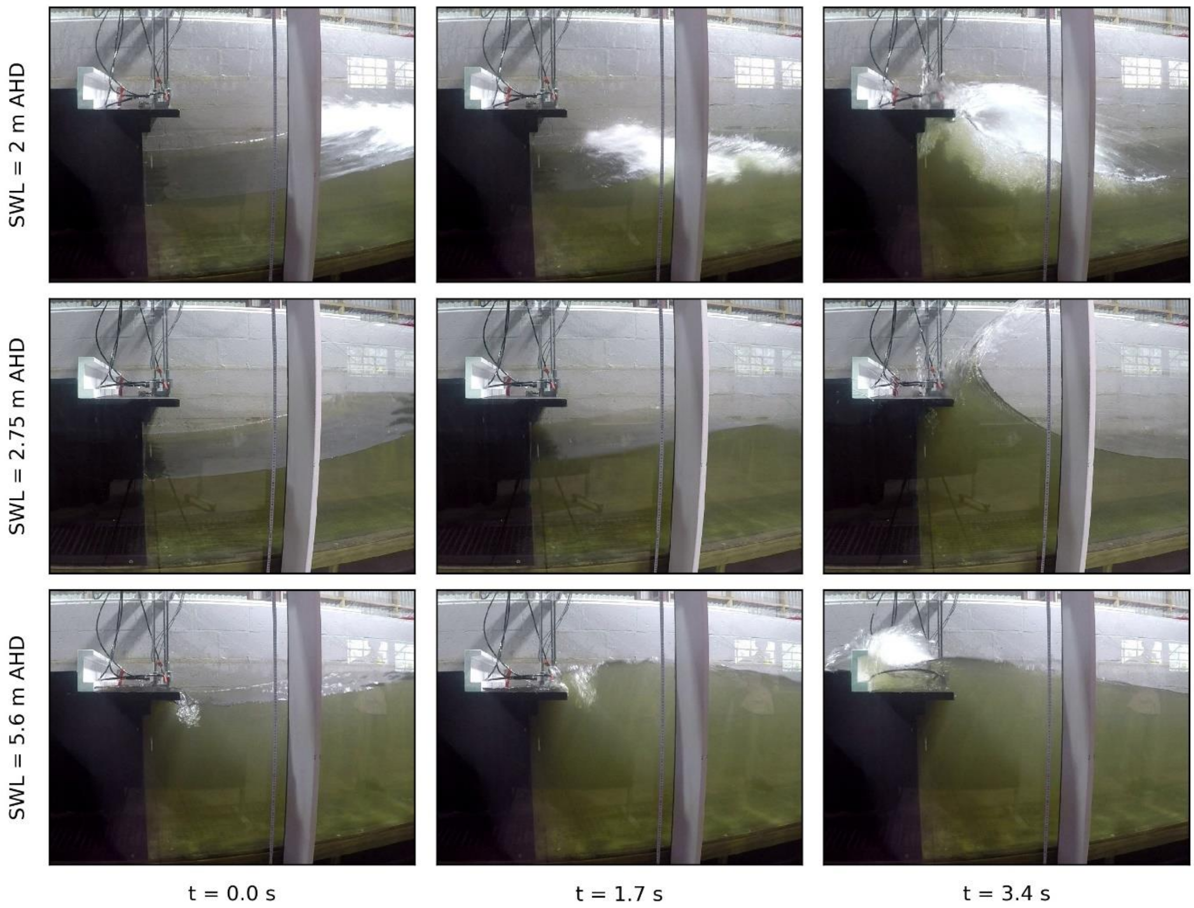

Figure 3-1 Waves impacting on the structure at different water levels

3.2 Forces

Forces were measured at each corner of the load-sensing section of the cantilevered walkway (Figure 2-4, Figure 2-5), which represented a 4.5 m long section of the walkway. The values from the four (4) load cells were summed to obtain the total force, and the peak total uplift force for each wave was identified (Figure 3-2). Total force peaks less than 100 kN over the 4.5 m long walkway section were not included in the analysis. An artefact of the load cell arrangement (four points of contact) is that a vertically upwards point load applied to one corner of the load-sensing section will result in a vertically downwards load being recorded at the diagonally opposite corner. As such, WRL recommends that the model results are used to determine the total force only (the instantaneous sum of the four load cells) rather than load distributions (e.g. individual load cells) across the wave flume or between the seaward or leeward edges of the cantilevered walkway.

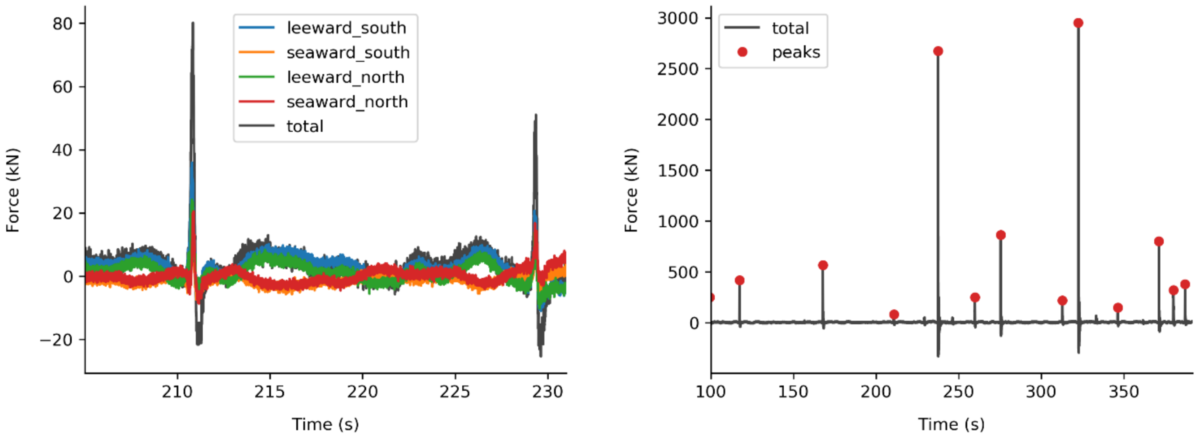

Figure 3-2 Calculation of total forces (left) and identification of peak forces (right) for test 7

Two parameters were used to compare the peak uplift forces between tests (Figure 3-3):

- F_{max}; and
- $F_{1/250}$ (the mean of peak values above the 1/250 level; the average of the four highest values recorded during each test of 1,000 waves).

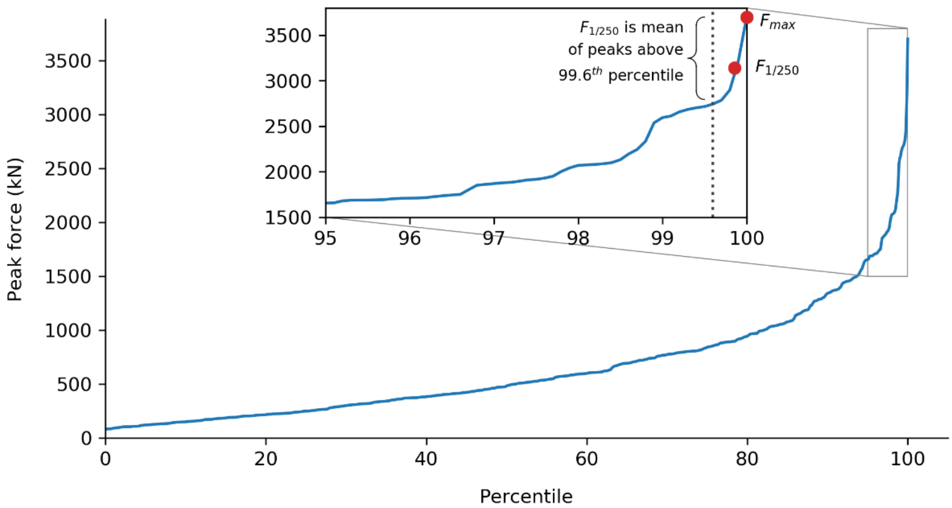

Figure 3-3 Distribution of total peak force and calculation of $F_{1/250}$ for test 7

3.3 Pressures

Pressures were measured at three locations on the underside of the fixed portion of the cantilevered walkway (Figure 2-4, Figure 2-5). Peak uplift pressures for each wave were identified for each sensor (Figure 3-4). Peak pressures less than 10 kPa were not included in the analysis.

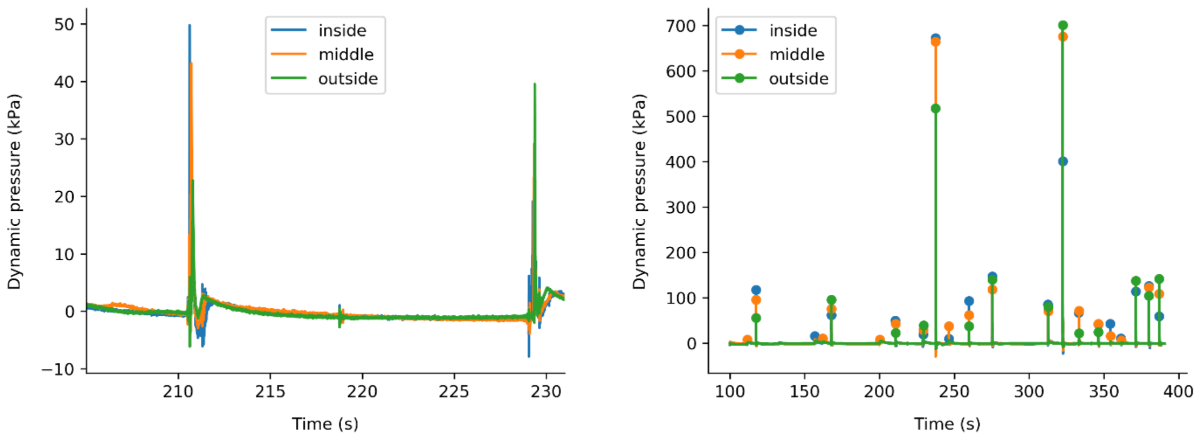

Figure 3-4 Pressure time series (left) and identification of peak pressures (right) for test 7

Measurements provided are dynamic pressures where the hydrostatic (still water) and barometric (ambient atmospheric) pressure are subtracted from the absolute (observed) pressure. Total water pressure can be calculated by adding the theoretical hydrostatic water pressure to the provided dynamic values (this conversion is only required for test 1 and test 18, when the pressure sensors were below still water level).

Unfortunately, some of the larger waves caused uplift pressures beyond the measurement range of the selected pressure sensors (approximately 700 kPa). These large pressures only occurred for a short time (approximately 20 ms), but the peak values were clipped from the signal (Figure 3-5).

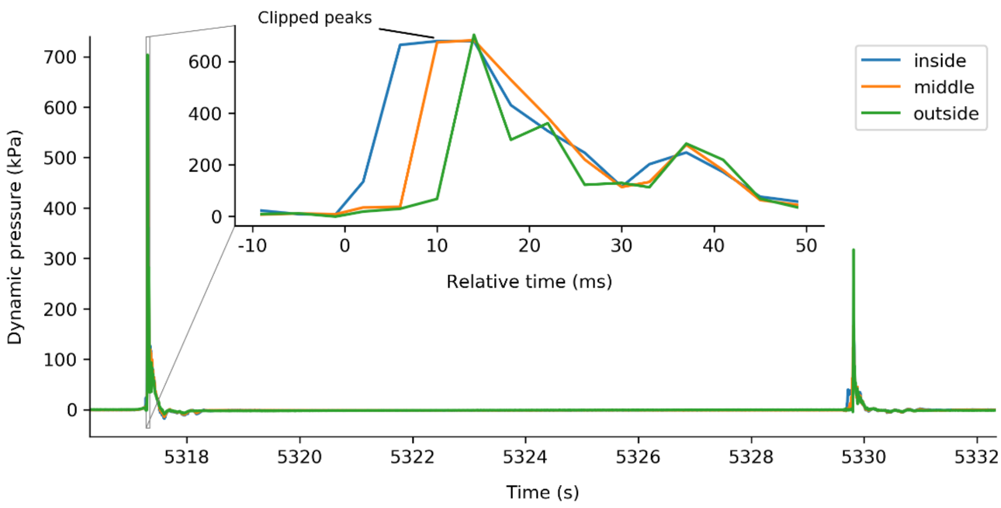

Figure 3-5 Example clipping of peak pressures in test 6

When this clipping was first observed, WRL consulted with WGA, and it was agreed to continue testing with the selected pressure transducers (rather than acquiring alternative units with a higher measurement range) as WGA's structural design would primarily be based on the load cell results rather than the pressure measurements.

Since pressure clipping was observed in most tests, P_{max} was not a useful measure to compare different test results. The 97th percentile pressure (P_{97}; Figure 3-6) was used instead because clipping was not observed at or below this percentile for all tests.

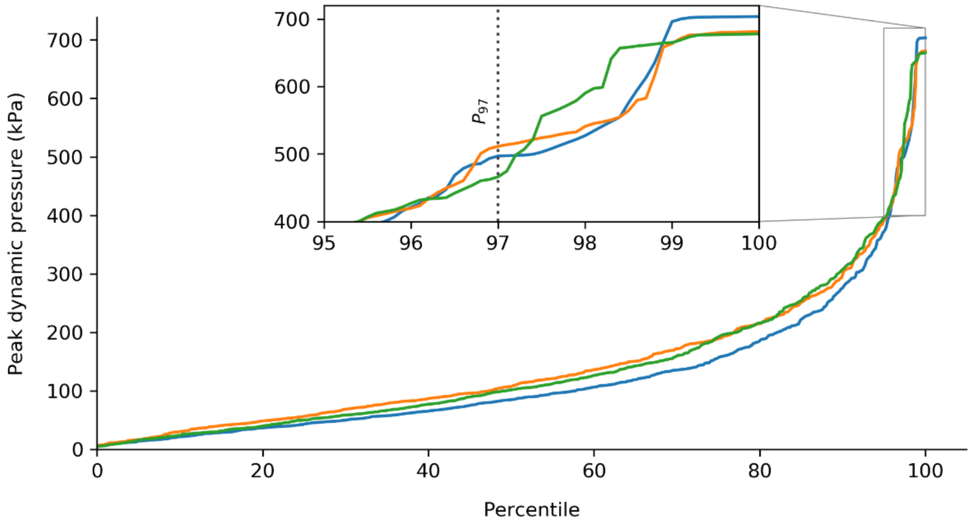

Figure 3-6 Distribution of peak pressures (note clipping above 98th percentile) for test 6

3.4 Peak uplift forces and pressures

The maximum peak uplift forces and pressures were observed at water levels between 2.4 m AHD and 3.0 m AHD (Figure 3-7, Figure 3-8). For tests between these water levels, the typical total duration (rise and fall) of the force and pressure impacts was approximately 0.2 to 0.3 s. A summary of peak forces and pressures is given in Table 3-2.

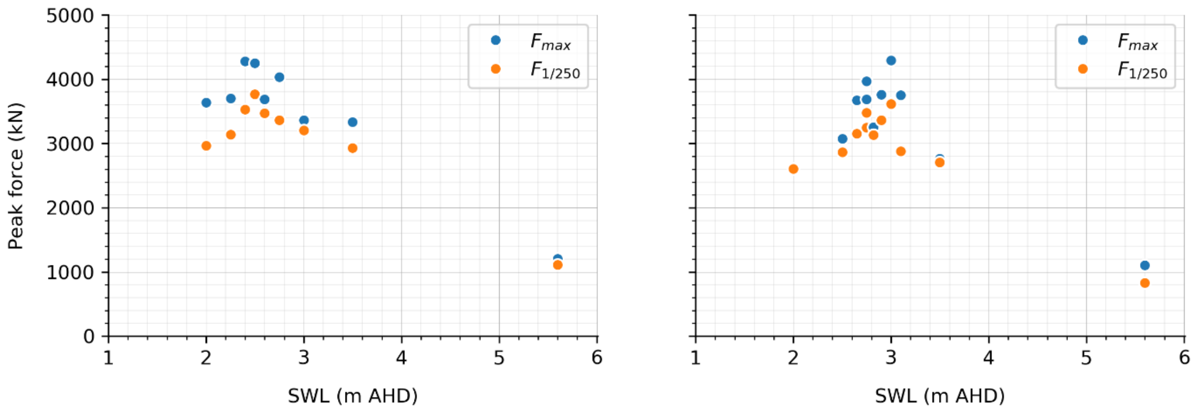

Figure 3-7 Peak force values (F_{max} and $F_{1/250}$) for different water levels (left: wave condition 1, right: wave condition 2)

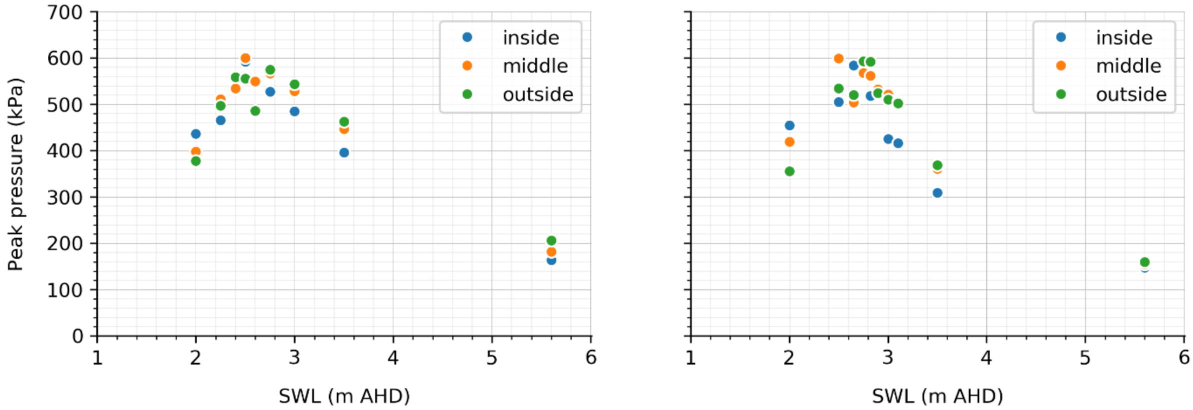

Figure 3-8 Peak pressure values (97th percentile) for different water levels (left: wave condition 1, right: wave condition 2)

Table 3-2 Peak total forces and pressures for all tests

Wave condition	Test number	SWL (m AHD)	Hs (m)	Tp (s)	Forces[1]		Pressures (97th percentile)		
					$F_{1/250}$ (kN)	F_{max} (kN)	Outside (kPa)	Middle (kPa)	Inside (kPa)
1	4	2.0	2.6	8.1	2965	3639	378	398	436
	7	2.25	2.6	8.1	3143	3701	497	511	466
	9	2.4	2.6	8.1	3533	4280	559	534	533
	6	2.5	2.6	8.1	3765	4248	556	600	592
	8	2.6	2.6	8.1	3474	3690	486	550	549
	3	2.75	2.6	8.1	3364	4038	575	566	528
	5	3.0	2.6	8.1	3203	3361	543	529	485
	2	3.5	2.6	8.1	2932	3334	463	447	396
	1	5.6	2.6	8.1	1111	1206	206	182	164
2	19	2.0	2.0	8.7	2607	2612	356	419	455
	10	2.5	2.0	8.7	2865	3071	535	600	505
	16	2.65	2.0	8.7	3153	3674	520	504	584
	11	2.75	2.0	8.7	3477	3688	593	568	564
	17	2.82	2.0	8.7	3133	3256	592	561	518
	14	2.9	2.0	8.7	3364	3761	525	532	528
	12	3.0	2.0	8.7	3619	4293	510	521	425
	15	3.1	2.0	8.7	2883	3754	502	506	416
	13	3.5	2.0	8.7	2710	2766	369	361	309
	18	5.6	2.0	8.7	829	1104	160	154	148

1. Force is distributed across a rectangular surface with length = 4.5 m and width = 1.43 m.

Wave condition 1 (H_s = 2.6 m, T_p = 8.1 s) recorded the peak uplift forces at water levels of 2.4 to 2.5 m AHD and wave condition 2 (H_s = 2.0 m, T_p = 8.7 s) had maximum uplift at the 3.0 m AHD water level. This difference in water level is likely to have occurred because wave condition 2 had a lower wave height and so a higher water level was required to achieve similar uplift dynamics. Regardless of this, the maximum recorded uplift force on the underside of the cantilevered walkway was nearly identical for wave condition 1 (4,280 kN) and wave condition 2 (4,293 kN).

4 Conclusion

WRL completed 2D physical modelling of a proposed vertical seawall with a cantilevered walkway, and measured uplift forces and pressures on the underside of the walkway deck to assist with WGA's structural design. The key objective of the model investigation was to estimate the maximum wave-generated uplift loads on the walkway for two different wave conditions, and to understand the influence of water level on the resulting wave loads.

Two different wave conditions were tested (H_s = 2.6 m, T_p = 8.1 s and H_s = 2.0 m, T_p = 8.7 s) at multiple water levels between 2.0 m AHD and 5.6 m AHD. The largest uplift forces and pressures were observed at water levels between 2.4 m AHD and 3.0 m AHD. The largest maximum peak force (F_{max}) measured was 4,293 kN, based on the sum of forces measured at four corners of a movable plate with dimensions 4.5 m x 1.43 m. The maximum peak pressures could not be accurately measured, because they exceeded the measurement range of the pressure sensors (approximately 700 kPa). The largest 97th percentile peak pressure measured was 600 kPa.

It should be noted that these 2D physical model tests represent a highly idealised case where the incident wave direction is exactly perpendicular to the alignment of the vertical seawall. In the real-world, some wave obliquity is likely to exist along the vertical seawall due to the variability of incident wave directions (i.e. directional spreading) and the partially curved planform of the seawall. At times, this phenomena was even observed in the 2D physical model where phase differences existed in force and pressure peaks due to small variations in the wave front across the flume (e.g. three-dimensional effects). For WGA's consideration of global loads on the cantilevered walkway, the peak loads measured in the physical model would only apply to relatively short sections at any given time (e.g. phase differences will exist for "impulsive" forces imparted along the length of the walkway).

5 References

BMT WBM 2017, *Darwin Luxury Hotel Seawall – Joint Probability of Elevated Water Level and Wave Report* R.B22260.001.01, Revision 1, 7 June 2017, BMT WBM Pty Ltd, Spring Hill, Australia.

BMT WBM 2018, *Darwin Luxury Hotel - Seawall – Marine Basis of Design Report* R.B22954.000.01, Revision 1, 22 May 2018, BMT WBM Pty Ltd, Spring Hill, Australia.

Bullock, G N, Crawford, A R, Hewson, P J, Walkden, M J A and Bird, P A D, 2001, 'The influence of air and scale on wave impact pressures', *Coastal Engineering*, 42(4), pp.291-312.

Bullock, G N, Obhrai, C, Müller, G, Wolters, G, Peregrine, D H and Bredmose, H, 2004, 'Characteristics and design implications of breaking wave impacts', Proc. Coastal Engineering 2004: (In 4 Volumes) (pp. 3966-3978).

Bullock, G N, Obhrai, C, Müller, G, Wolters, G, Peregrine, D H and Bredmose, H, 2005, 'Advances in the understanding of wave-impact forces'. *Proc. Coastlines, Structures and Breakwaters*, London: Thomas Telford, pp.111-120.

Bullock, G N, Obhrai, C, Peregrine, D H and Bredmose, H 2007, 'Violent breaking wave impacts. Part 1: Results from large-scale regular wave tests on vertical and sloping walls', *Coastal Engineering*, 54(8), pp.602-617.

Cuomo, G, Allsop, W and Takahashi, S 2010, 'Scaling wave impact pressures on vertical walls', *Coastal Engineering*, 57(6), pp.604-609.

Hughes, S A 1993, *Physical models and laboratory techniques in coastal engineering*, Advanced Series on Ocean Engineering, World Scientific, USA.

Hydralab III 2007, Wolters, G, Van Gent, M R A, Mühlestein, D, Kirkegaard, J, Allsop, W, Gironella, X, Fortes, J, Capitão, R, Sousa, I, Pinheiro, L, Santos, J, Hamm, L and Bonthoux, L, *Guidelines for Physical Model Testing of Breakwaters: Rubble Mound Breakwaters*, Deliverable NA3.1-2, Final Report (Version 1.3), European Commission.

Mansard and Funke 1980, The measurement of incident and reflected spectra using a least squares method, *Proceedings of the 17th Coastal Engineering Conference*, 1 (1980), pp. 154-172

McMahon Services 2019, Re: Darwin Seawall Bathymetry – 180954, [E-mail], Message from G Solly (garry.solly@mcmservices.com.au) to I R Coghlan (i.coghlan@wrl.unsw.edu.au). Sent 21/08/2019 10:08 AM

QGHL 2017, *Darwin Hotel Seawall, Physical modelling of a vertical piled seawall*, Queensland Government Hydraulics Laboratory, Department of Science, Information Technology and Innovation, Brisbane Australia, December, 2017.

Ramkema, C 1978, 'A Model Law for Wave Impacts on Coastal Structures', *Proc. Coastal Engineering Conference*, Hamburg, Germany.

Robert Bird Group 2018, "Seawall Enabling Works: Sections Sheet 1", Drawing no. RBG-CV-DRW-A0036, Revision E ("Approved For Construction"), 19 December 2018, AutoCAD drawing.

Van Gent, M R and Giarrusso, C C 2005, 'Influence of foreshore mobility on wave boundary conditions', *Proc. International Conference on Ocean Waves Measurements and Analysis*, Madrid, Spain (pp. 3-7), July 2005.

Appendix A Vertical Seawall Design Drawing (Robert Bird Group, 2018)